

Article

Battery-Free Shape Memory Alloy Antennas for Detection and Recording of Peak Temperature Activity

Wei Wang , Wenxin Zeng  and Sameer Sonkusale * 

Nano Lab, Electrical and Computer Engineering, Tufts University, Medford, MA 02155, USA;
wei.wang@tufts.edu (W.W.); wenxin.zeng@tufts.edu (W.Z.)

* Correspondence:sameer@ece.tufts.edu

Abstract: Economical sensing and recording of temperatures are important for monitoring the supply chain. Existing approaches measure the entire temperature profile over time using electronic devices running on a battery. This paper presents a simple, intelligent, battery-free solution for capturing key temperature events using the natural thermo-mechanical state of a Shape Memory Alloy (SMA). This approach utilizes the temperature-induced irreversible mechanical deformation of the SMA as a natural way to capture the temperature history without the need for electronic data logging. In this article, two-way SMA is used to record both high-temperature and low-temperature peak events. Precise thermo-mechanically trained SMA are employed as arms of the dipole antenna for Radio Frequency (RF) readout. The fabricated antenna sensor works at 1 GHz and achieves a sensitivity of 0.24 dB/°C and -0.16 dB/°C for recording temperature maxima and minima, respectively.

Keywords: antenna; battery-free; memory; temperature; two-way memory effect; Shape Memory Alloy



Citation: Wang, W.; Zeng, W.; Sonkusale, S. Battery-Free Shape-Memory Alloy Antennas for Detection and Recording of Peak Temperature Activity. *Crystals* **2022**, *12*, 86. <https://doi.org/10.3390/cryst12010086>

Academic Editor: Arcady Zhukov

Received: 12 December 2021

Accepted: 7 January 2022

Published: 9 January 2022

Publisher's Note: MDPI stays neutral with regard to jurisdictional claims in published maps and institutional affiliations.



Copyright: © 2022 by the authors. Licensee MDPI, Basel, Switzerland. This article is an open access article distributed under the terms and conditions of the Creative Commons Attribution (CC BY) license (<https://creativecommons.org/licenses/by/4.0/>).

1. Introduction

Managing temperature is one of the biggest challenges for the supply chain, especially for health and pharmaceutical goods [1]. Even short-term exposure to heat can reduce the efficacy of drugs. To ensure the quality of temperature-sensitive pharmaceuticals, refrigeration and cold chain management are required [2]. While high temperatures are considered detrimental, it is known that extremely low temperatures can also compromise drug efficacy (e.g., freezing of vaccines in the cold chain) [3]. Freeze-sensitive vaccine loses its potency when the temperature is below the recommended range, and such a scenario can result in a false sense of potency and put people's lives at risk with ineffective vaccines. Thus, monitoring of extreme temperature events, both high and low, during the supply chain is of paramount importance in the pharmaceutical supply chain. Conventional monitoring methods that continuously sense the temperature and record the entire temperature history require circuitry for continuous acquisition, electronic memory to store the data, and a dedicated battery, making it bulky and expensive. Sensors that do not rely on a battery offer great promise in such a scenario. There has been a trend to rely on the material properties of sensors to detect and record the relevant events without any power sources. Temperature-induced irreversible mechanical deformation of Shape Memory Alloy (SMA) has been used to capture real-time temperature [4] and of extreme high and low levels [5]. Shape-morphing, cold-temperature-reactive Liquid Crystal Elastomers (LCEs) have been used to detect temperature threshold crossings for multiple temperature cycles [6]. Recording a singular event of temperature crossing with liquid metal coupled to a Radio-Frequency Identification (RFID) tag was reported in [7]. The crossing of a temperature threshold results in liquid metal flow, which activates or deactivates the RFID tag permanently. In another work, a thermistor resistor was used as a switch along with an RFID tag to wirelessly detect the temperature profile [8,9]. RFID technology has also been used in conjunction with the bimetallic coil as a passive digital sensor for temperature without the need for battery [10]. A tilt sensor coupled with an RFID tag has also been used

for home security sensing in prior work [11,12]. In related work, e-textile and conductive thread material have been seamlessly integrated into clothing for human activity sensing by detecting different backscatter signal strengths [13–16]. E-textile has also been used to sense humidity by detecting different backscatter signal strengths [17–19]. Some other applications of RFID include battery-less RFID thread [20,21] and MagRFID sensor [22], which have been utilized for tamper-detection monitoring and security monitoring.

Similarly, we propose zero-power low-cost temperature sensors that monitor extreme temperature events for pharmaceutical supply chain monitoring. Note that monitoring critical temperature-crossing events rather than real-time temperature information will reduce data complexity and overall power consumption. Figure 1 shows our proposed design, where the temperature sensors are attached to each package to record individual extreme temperature activity. During transportation, as the temperature fluctuates, the battery-free sensor records the peak temperature information. The sensor itself consists simply of a temperature-sensitive antenna, where peak temperature events are naturally stored in the geometric configuration of the antenna. No other circuitry or memory element is needed for sensing. An external radiofrequency (RF) reader is connected to the sensor at any time to read the antenna response that depends on historical peak temperatures experienced by the package. One can also connect the antenna to a wireless RF module for wireless readout, which will be the basis for future work.

The design of the temperature-sensitive antenna relies on a two-way SMA as arms of temperature-sensitive antennas to support easy read-out. Using a two-way SMA, a temperature sensor can track the peak temperature activity and record the highest or lowest temperature it has experienced. It operates without power resources during the supply chain, which greatly reduces the cost and makes this platform scalable for tracking many temperature-sensitive applications.

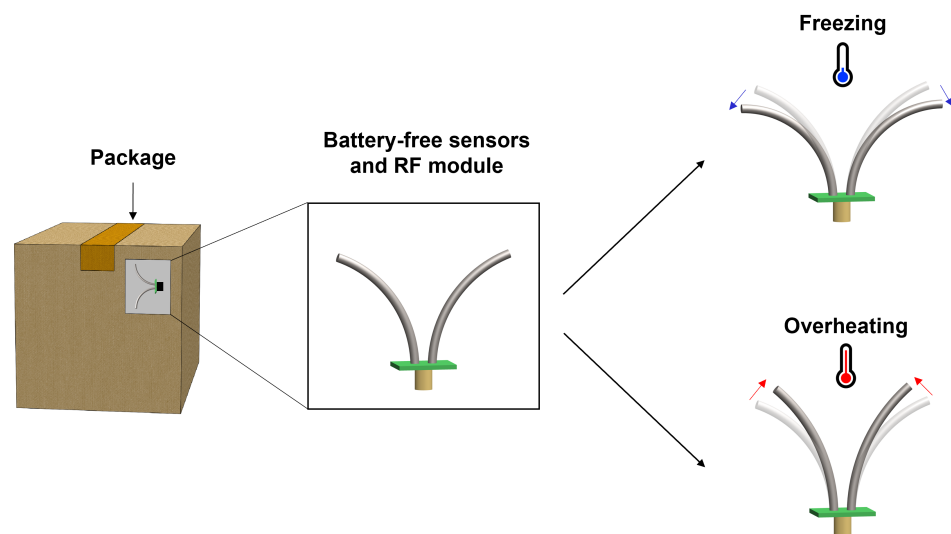


Figure 1. Battery-free shape memory alloy antenna sensors that record the critical temperature information during transportation.

2. Background on Shape Memory Alloys

SMA is metal alloys that transform their mechanical properties with temperature. With its intrinsic thermo-mechanical memory, the SMA can alter its shape when the temperature reaches certain thresholds. The SMA is under an austenite state when the temperature is above the threshold, in which case the molecules are tightly patterned and the SMA is rigid. When the temperature is below the threshold, the molecules become loose and the SMA is in a martensite state. An SMA has either a one-way memory effect or a two-way memory effect depending on the training state. For the one-way memory effect, an SMA has three crystal structures (austenite, twinned martensite, and detwinned martensite), as indicated in Figure 2a. When the temperature is above the threshold, the SMA is in a

rigid austenite phase. When the temperature drops below the threshold, the SMA switches to the martensite phase, where the atoms can be re-arranged in a loose pattern so that the SMA is more pliable. If no external stress is applied to the SMA, its crystal structure stays in a twinned martensite state, and its overall shape is the same as the austenite phase. If external stress is applied, the SMA is reshaped by the force, and its crystal structure becomes a detwinned martensite state. Once the SMA returns from a detwinned martensite state to an austenite state when the temperature rises above the threshold, it recovers to its originally predefined shape. From a crystallographic viewpoint, the heat energy leads to the reorientation of SMA atoms to the symmetric pattern. From the macroscopic view, this reorientation results in the recovery of the predefined physical shape once it reaches a high temperature. This self-recovering process is irreversible, that the austenite state cannot return to the detwinned martensite state without external stress. Thus, a one-way SMA has built-in memory to remember the predefined high-temperature configuration. A two-way SMA, however, has the memory effect in both directions. The critical start and end temperatures of forming the martensite phase and austenite phase for two-way SMAs are defined as M_s , M_f , A_s , and A_f , respectively. The SMA starts to alter its phase from martensite to austenite at temperature A_s and finishes the transition at A_f , along with its shape; similarly, changing from austenite to martensite begins at temperature M_s and finished at M_f , as shown in Figure 2b [23].

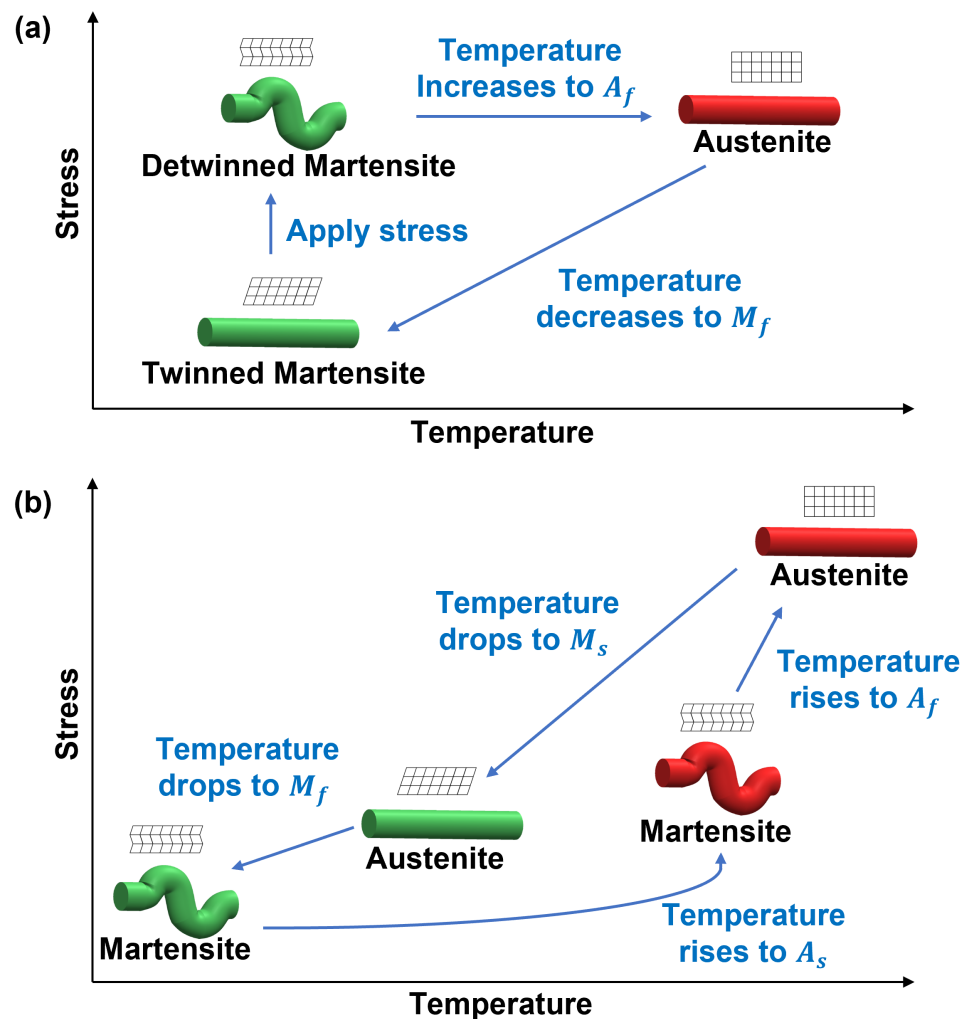


Figure 2. (a) Phase shift of one-way SMA and (b) phase shift of two-way SMA.

As alluded to in the introduction, we present a peak temperature sensing and recording approach using a shape-memory alloy-based antenna. In realization, SMA is assembled as arms of temperature-sensitive antennas that deform as a function of temperature. Each of the SMA arms will have undergone controlled thermo-mechanical training as a function of temperature. This imparts the SMA with a specific and characteristic temperature-sensitive mechanical deformation that can be used for sensing temperature.

3. Peak Temperature Recording Antenna Using Two-Way SMA

SMA has been used for tunable antennas [24], threshold temperature [4], and peak temperature with visual readout [5], and actuator [25,26]. In this article, a temperature-sensitive antenna is fabricated with two-way SMA for sensing and recording the peak temperature information with a radio frequency (not visual) readout. The operation of the SMA antenna sensor for tracking the highest environmental temperature is shown in Figure 3a; the black curve shows the real-time temperature, and the red-color curve tracks the recorded highest temperature T_1 stored in the thermomechanical shape of the antenna. As the environmental temperature drops, the red curve shows the thermomechanical shape corresponding to the highest temperature value. The arms of the antenna are made such that it has a predefined large opening angle at the low temperature and a small opening angle at the high temperature. Assume, initially, that the antenna is placed in a low temperature T_0 , and it presents a low-temperature predefined configuration with a large open angle, as in Figure 3b. As the temperature increases, it gradually changes its shape towards the high-temperature predefined configuration, and the opening angle decreases. At the highest temperature T_1 , the antenna presents a small opening angle as in Figure 3c, and it remains this configuration even if the temperature drops below T_1 in the future, as shown in Figure 3d. Conversely, for tracking the lowest environmental temperature, as in Figure 3e, the black curve shows the real-time temperature, and the blue curve tracks the thermomechanical shape for the lowest temperature it experienced. If the environmental temperature rises above the lowest temperature, the blue curve keeps the configuration for the lowest temperature value. Assume the antenna sensor is initially placed in a high temperature T_3 so that it is in a high-temperature predefined configuration with a small open angle, as in Figure 3f. It will gradually change towards the low-temperature predefined configuration as the temperature falls, leading to a gradually larger opening angle. At the lowest temperature, T_4 , the antenna presents the largest opening angle, as shown in Figure 3g. In this process, even if the temperature rises above T_4 , the two-way SMA remains the configuration of the lowest temperature it experiences, as indicated conceptually in Figure 3h. Therefore, depending on the initial temperature setting, the antenna can be used to record the highest or lowest temperature it experiences. The antenna-based sensor automatically filters the nominal temperature information and only keeps the peak temperature data. Different peak temperatures induce different geometric profiles of the antenna. The shape and dimensions of the antenna dictate the frequency-dependent current density, which influences the radiation profile and alters the antenna parameters such as directivity and gain [27]. Therefore, sensing the radiation profiles from the antenna, such as through measurement of S_{11} , a measure of power at the input (reflected power), the peak temperature information can be obtained without the need for real-time temperature sensing or data logging.

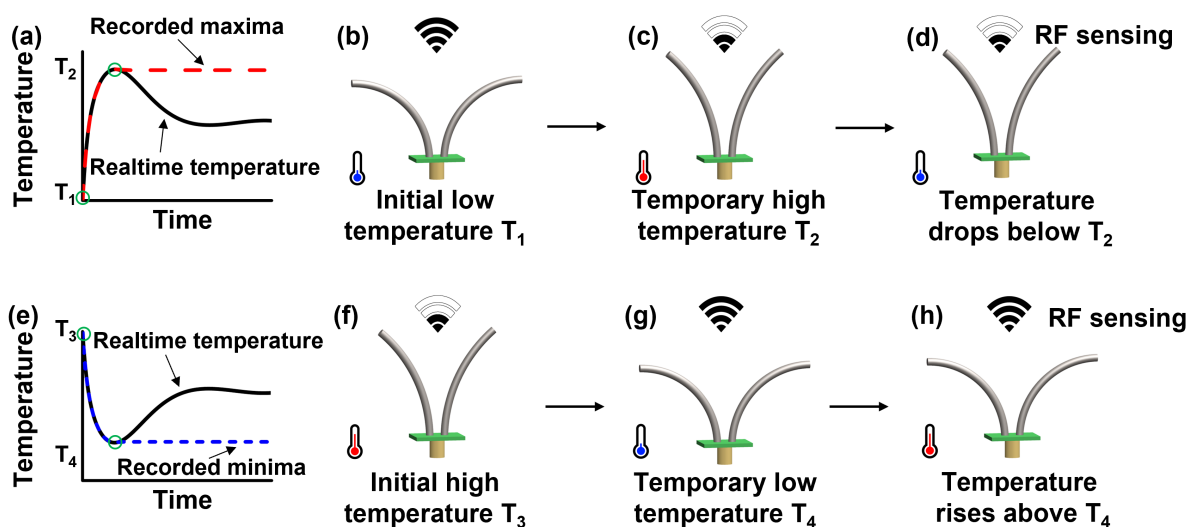


Figure 3. (a) SMA antenna records the maximum history temperature. (b) Antenna presents a large opening angle at an initial low temperature. (c) Antenna presents a small opening angle at the highest temperature. (d) Antenna keeps the small opening angle when the temperature drops. (e) SMA antenna records the minimal history temperature. (f) Antenna present a small opening angle at an initial high temperature. (g) Antenna presents a large opening angle at the lowest temperature. (h) Antenna keeps the large opening angle when the temperature increases.

4. Experiment Results

To apply the temperature extrema antenna sensor in the supply chain, we choose SMA wires with A_s and A_f being 20 °C and 40 °C, and M_s and M_f being 10 °C and −10 °C. In real practice, the temperature range should be chosen such that it matches the recommended storage temperature range of the drug/pharmaceutical being monitored. The fabricated sensors can be placed on the packages for individual monitoring. Before deploying the sensors into the supply chain, the SMA-based sensor can be cooled below M_f , in our case, at a temperature of −15 °C, to prime the sensor to track the highest temperature. As the temperature varies, the SMA will change its configuration, and assuming the highest temperature of the package reaches 30 °C, the two-way SMA wire will lock its configuration based on this highest temperature it experienced, even if the temperature drops later to, e.g., 10 °C. Similarly, if the initial temperature is set higher than A_f , the two-way SMA wire has a high-temperature predefined configuration. It can be used to record the lowest temperature of the package in a manner analogous to what was discussed above for high peak temperature recording, albeit the difference here is the shape tracks the lowest experienced temperature. An RF-based readout can be used where the two-way SMA performs as arms of the antenna, and the radiation intensity or pattern is monitored as the indicator of peak temperature. The two-way memory effect with user-defined temperature settings is obtained with a thermo-mechanical training process. The below describes this training process to form the two-way SMA [5,28].

4.1. Forming High-Temperature Predefined Configuration

We use nickel–titanium alloy SMA wires (Nexmetal) with a diameter of 0.5 mm. The first step is to program the shape or configuration that the SMA wire will acquire at high temperatures. This is achieved by manually shaping the SMA wire in this high-temperature predefined configuration. While being constricted in this shape, the SMA wire is then annealed in a furnace at 300 °C for around 10 min. Sustained high-temperature exposure permanently rearranges the lattice structure realizing a one-way memory; this predefined structure will be the one for which the SMA recovers when heated.

4.2. Forming Low-Temperature Predefined Configuration

To program the shape or configuration that the SMA will acquire at low temperature, the SMA is firstly cooled in an icy bath. The low-temperature environment brings the SMA wire into the martensite state, in which the SMA is pliable. The SMA is folded into a spring shape beyond its usual strain limit in the icy water of 5 °C or 5 min, as in Figure 4a. This step locks in the second recoverable shape of the SMA at a low temperature. The SMA is then transferred to a hot bath with a temperature around 60 °C, causing the shape to recover to the high-temperature predefined shape as in Figure 4b.

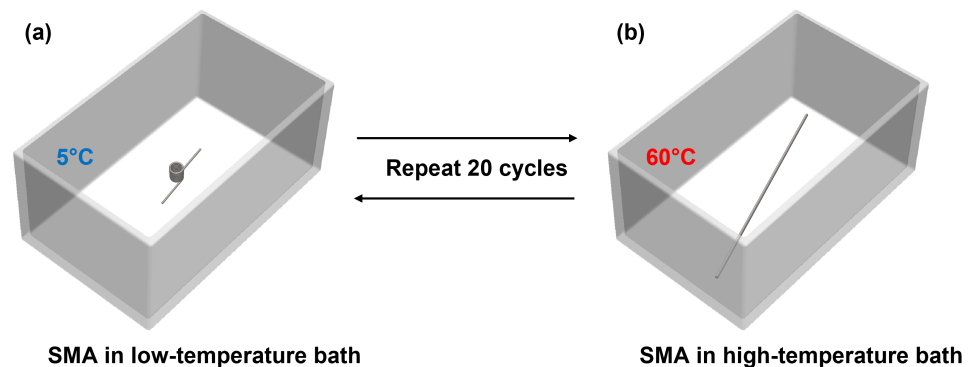


Figure 4. Thermo-mechanical training of the two-way SMA. (a) SMA is in low-temperature bath for training. (b) SMA is in high-temperature bath for training.

The above steps are repeated for 20 cycles. This results in the formation of a two-way SMA. Heating or cooling causes the SMA to spontaneously change shape to the direction in which it has been consistently deformed. Note that the amount of the shape change on cooling will be significantly less than what was induced during the thermo-mechanical training steps mentioned above, and the recovery at high temperatures may be incomplete compared to the original straight-line configuration due to the excessive deformation in the martensite phase. However, the platform's extreme temperature behavior is adequately distinct and repeatable for temperature sensing.

To make a temperature-sensitive antenna, two trained SMA wires are soldered onto a tiny Print Circuit Board (PCB). The PCB works as a simple frame for the SMA wires to be soldered on and connects the SMA wires to a signal connector. Figure 5 shows the configuration that the antenna changes to as temperature increases from 23 °C to 40 °C in a temperature-controlled chamber. A vector network analyzer (Agilent N5227A) is used to measure the return loss S_{11} . First, S_{11} around 1 GHz is recorded while the temperature gradually increases from −20 °C to 50 °C. The fabricated antenna was placed inside a custom RF anechoic chamber. The chamber works as both an RF signal absorber and a thermal insulator. A small heater and dry ice were used for heating and cooling, respectively. For the heating process, the chamber was first cooled by putting the dry ice inside, and then the heater slowly increased the temperature in the chamber. This results in a smaller opening angle formed by the two arms of the antenna. During this process, S_{11} and temperature are recorded simultaneously. Second, the temperature is gradually decreased from 50 °C to −20 °C, leading to a larger opening angle of the antenna. The chamber is preheated to 50 °C with the small heater and then cooled by dry ice. The cooling process leads to a larger opening angle of the antenna. Temperature and S_{11} monitoring are also performed similarly for the cooling process. The physical length of the antenna is the same in different shapes. Therefore, the resonant frequency does not change as much. However, different opening angles lead to different radiation patterns due to different antenna impedance and thus different S_{11} values, as shown in Figure 6a,b. For the rising temperature process shown in Figure 6a, the return loss around 1 GHz at 30 °C is −11 dB. When the temperature rises to 47 °C, the return loss is reduced to −7 dB due to the more closed antenna shape. Note that the return loss to temperature conversion is not linear and

the antenna is most sensitive around 39 to 44 °C. The average sensitivity over the entire temperature range is roughly 0.24 dB/°C. Similarly, for the decreasing temperature process shown in Figure 6b, the return loss around 1 GHz at 13 °C is −6.5 dB and is −11.4 dB at −17 °C. The result shows a similar non-linearity and is most sensitive around −7 to 3 °C. The average sensitivity around the entire range is −0.16 dB/°C.

The ability to hold the information of the highest or lowest temperature is also tested. Three sets of two-way SMA antennas are initially set at −20 °C. The temperature is gradually increased to 36 °C, 39 °C, and 42 °C, respectively, and then decreased. The shape of the antenna and the peak of S_{11} remain the same value measured at the previous high temperature, even when the temperature drops, as shown in Figure 6c. The time when each measurement is taken is also shown in the figure. Similar tests are done in a decreasing-temperature situation, where the temperature drops to 4 °C, −2 °C, and −12 °C, respectively, and then rises back. The peak of S_{11} remains the same value it had measured at the previous lowest temperature, as shown in Figure 6d.

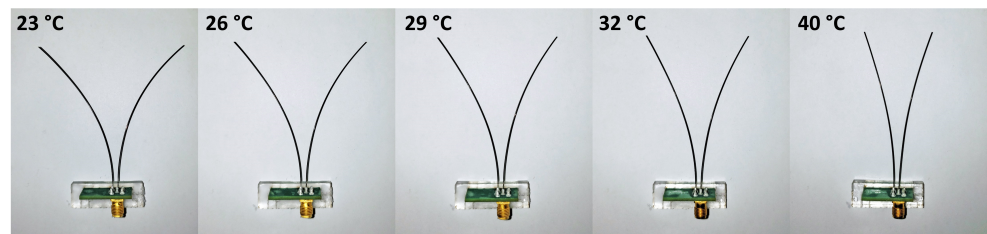


Figure 5. SMA antenna presents different shape at 23 °C, 26 °C, 29 °C, 32 °C and 40 °C.

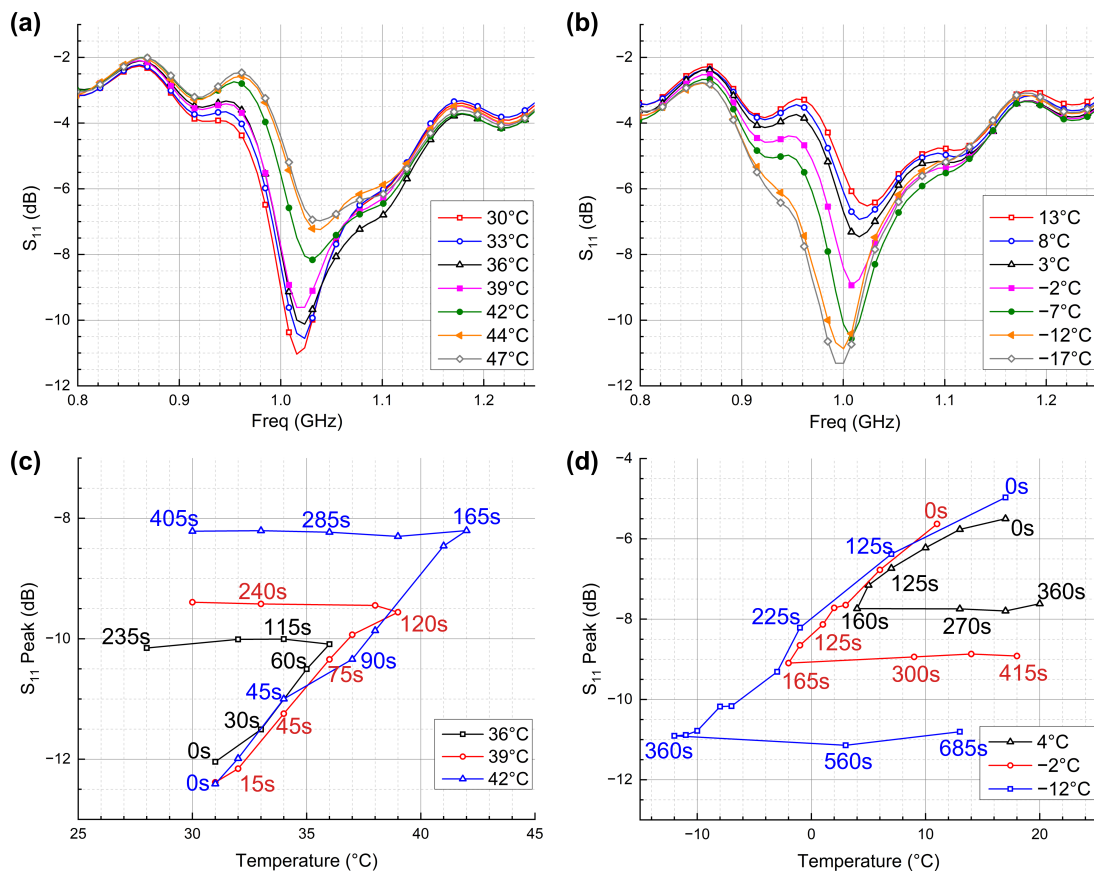


Figure 6. Return loss S_{11} of two-way SMA under (a) heating and (b) cooling process; and peak value of S_{11} when two-way SMA are (c) heated and (d) cooled to different temperatures.

The minimal value of S_{11} during the temperature sweep is extracted and plotted in Figure 7. It shows the hysteretic nature of the SMA, which plays a critical role in

recording the highest or lowest temperature. When the temperature changes from $-15\text{ }^{\circ}\text{C}$ to $60\text{ }^{\circ}\text{C}$, the SMA configuration changes gradually so that at each temperature point, there is a corresponding unique physical configuration. Different configurations of the antenna result in different return loss S_{11} , providing a readout of temperature from the antenna configuration.

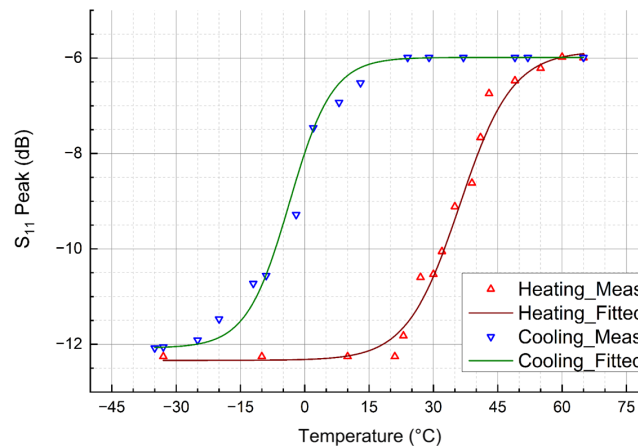


Figure 7. Minimal value of S_{11} during the temperature sweep.

5. Discussion

Note that if the temperature variation is within the hysteresis, the sensor will record only the maxima or minima, no matter how many local maxima or minima it has experienced. It can only detect one extremity, and this value is set before the application through the SMA's thermomechanical training. If both maxima and minima are needed, two sensors are required. If the temperature variation is beyond the hysteresis, the sensor will not work to record activity beyond the hysteresis range. In this case, SMA wires with different temperature thresholds to cover the temperature range will be required. We assume that the users will know the temperature range of their application and proper SMA wires with appropriate temperature profiles will be chosen accordingly. Achieving a wider temperature range using multiple SMA antennas could be the focus of the future work.

The sensor has a response time, typically less than one second. If the temperature change is faster than the sensor response time, then the sensor will not change its configuration. For the typical applications in monitoring the temperature of goods during transportation, the sensor response time is much faster than the anticipated temperature change.

The SMA can hold its shape in this application since the weight of the SMA wire is negligible and is taken into account through thermomechanical training. We do not expect to subject the antenna to any additional weight. If the antenna is deformed due to mechanical force by accident, it may change the shape of the SMA wire temporarily, which will recover when stabilized when SMA is adequately thermo-mechanically trained.

6. Conclusions

This paper presents a simple battery-free approach to sense peak temperature information using the natural phase-change property of shape memory alloys or SMAs. We present a thermo-mechanical programming process to realize two-way SMA that can sense and record the peak temperature information. One can track historical peak temperature activity using a single passive device without any onboard power source or electronic circuitry such as memory or microcontrollers. The readout can be done at any time in the future using an RF reader. While not demonstrated here, one can achieve wireless readout using a passive RF module and an RF reader at the transportation terminals. The whole sensor platform is low in cost, compact, and scalable to monitor individual packages in the supply chain.

Author Contributions: Conceptualization, W.W. and S.S.; methodology, W.W., W.Z. and S.S.; software, W.W. and W.Z.; validation, W.Z.; formal analysis, W.W., W.Z. and S.S.; investigation, W.W., W.Z. and S.S.; resources, W.W., W.Z. and S.S.; data curation, W.Z.; writing—original draft preparation, W.W. and W.Z.; writing—W.W., W.Z. and S.S.; visualization, W.W., W.Z. and S.S.; supervision, S.S.; project administration, S.S. All authors have read and agreed to the published version of the manuscript.

Funding: Authors would like to acknowledge partial funding from National Science Foundation (NSF) grants 1931978, 1951104, 1808912 and 1935555.

Institutional Review Board Statement: Not applicable.

Informed Consent Statement: Not applicable.

Conflicts of Interest: The authors declare no conflict of interest.

Abbreviation

SMA Shape Memory Alloy

References

- Privett, N.; Gonsalvez, D. The top ten global health supply chain issues: Perspectives from the field. *Oper. Res. Health Care* **2014**, *3*, 226–230. [[CrossRef](#)]
- Bishara, R.H. Cold chain management—An essential component of the global pharmaceutical supply chain. *Am. Pharm. Rev.* **2006**, *9*, 105–109.
- Hanson, C.M.; George, A.M.; Sawadogo, A.; Schreiber, B. Is freezing in the vaccine cold chain an ongoing issue? A literature review. *Vaccine* **2017**, *35*, 2127–2133. [[CrossRef](#)]
- Wang, W.; Zeng, W.; Sadeqi, A.; Sonkusale, S. Wireless Temperature Monitoring with Shape Memory Alloy-based Antenna. *IEEE Antennas Wirel. Propag. Lett.* **2021**, *20*, 313–336. [[CrossRef](#)]
- Wang, W.; Zeng, W.; Ruan, W.; Miller, E.; Sonkusale, S. Thermo-Mechanically Trained Shape Memory Alloy for Temperature Recording with Visual Readout. *IEEE Sens. Lett.* **2021**, *5*, 2500104. [[CrossRef](#)]
- Wang, W.; Owyung, R.; Sadeqi, A.; Sonkusale, S. Single Event Recording of of Temperature and Tilt Using Liquid Metal with RFID Tags. *IEEE Sens. J.* **2020**, *20*, 3249–3256. [[CrossRef](#)]
- Shafiq, Y.; Henricks, J.; Ambulo, C.P.; Ware, T.H.; Georgakopoulos, S.V. A Passive RFID temperature sensing antenna with liquid crystal elastomer switching. *IEEE Access* **2021**, *8*, 24443–24456. [[CrossRef](#)]
- Wang, W.; Asci, C.; Zeng, W.; Sonkusael, S. Zero-Power Screen Printed Flexible RFID Sensors for Smart Home. *Meas. Sci. Technol.* **2022**, *in press*.
- Hussein, H.; Rinaldi, M.; Onabajo, M.; Cassella, C. A chip-less and battery-less subharmonic tag for wireless sensing with parametrically enhanced sensitivity and dynamic range. *Sci. Rep.* **2021**, *11*, 3782. [[CrossRef](#)]
- Zhu, W.; Zhang, Q.; Matlin, M.; Chen, Y.; Wu, Y.; Zhu, X.; Zhao, H.; Pollack, R.; Xiao, H. Passive Digital Sensing Method and Its Implementation on Passive RFID Temperature Sensors. *IEEE Sens. J.* **2021**, *21*, 4793–4800. [[CrossRef](#)]
- Chen, X.; Feng, D.; Takeda, S.; Kagoshima, K.; Umehiras, M. Experimental validation of a new measurement metric for radiofrequency identification-based shock-sensor systems. *IEEE J. Radio Freq. Identif.* **2018**, *2*, 206–209. [[CrossRef](#)]
- Rahmadya, B.; Chen, X.; Takeda, S.; Kagoshima, K.; Umehira, M.; Kurosaki, W. Measurement of a UHF RFID-Based Battery-Less Vibration Frequency Sensitive Sensor Tag Using Tilt/Vibration Switches. *IEEE Sens. J.* **2020**, *20*, 9901–9909. [[CrossRef](#)]
- Liu, Y.; Yu, M.; Xia, B.; Wang, S.; Wang, M.; Chen, M.; Dai, S.; Wang, T.; Ye, T. E-Textile Battery-Less Displacement and Strain Sensor for Human Activities Tracking. *IEEE Internet Things J.* **2021**, *8*, 16486–16497. [[CrossRef](#)]
- He, H.; Chen, X.; Ukkonen, L.; Virkki, J. Clothing-integrated passive RFID strain sensor platform for body movement-based controlling. In Proceedings of the 2019 IEEE International Conference on RFID Technology and Applications (RFID-TA), Pisa, Italy, 25–27 September 2019.
- Mehmood, A.; He, H.; Chen, X.; Merilampi, S.; Sydanheimo, L.; Ukkonen, L.; Virkki, J. Body Movement-Based Controlling Through Passive RFID Integrated Into Clothing. *IEEE J. Radio Freq. Identif.* **2020**, *4*, 414–419. [[CrossRef](#)]
- Lin, R.; Kim, H.; Achavananthadith, S.; Kurt, S.; Tan, S.; Yao, H.; Tee, B.; Lee, J.; Ho, J. Wireless battery-free body sensor networks using near-field-enabled clothing. *Nat. Commun.* **2020**, *11*, 444. [[CrossRef](#)]
- Chen, X.; He, H.; Khan, Z.; Sydanheimo, L.; Ukkonen, L.; Virkki, J. Textile-based batteryless moisture sensor. *IEEE Antennas Wirel. Propag. Lett.* **2020**, *19*, 198–200. [[CrossRef](#)]
- Sen, P.; Kantareddy, S.N.R.; Bhattacharyya, R.; Sarma, S.E.; Siegel, J.E. Low-Cost Diaper Wetness Detection Using Hydrogel-Based RFID Tags. *IEEE Sens. J.* **2020**, *20*, 3293–3302. [[CrossRef](#)]
- Feng, Y.; Xie, L.; Chen, Q.; Zheng, L. Low-cost printed chipless RFID humidity sensor tag for intelligent packaging. *IEEE Sens. J.* **2015**, *15*, 3201–3208. [[CrossRef](#)]
- Wang, W.; Sadeqi, A.; Sonkusale, S. All-around Package Security Using Radio Frequency Identification Threads. In Proceedings of the IEEE Sensors, New Delhi, India, 28–31 October 2018.

21. Wang, W.; Sadeqi, A.; Nejad, H.R.; Sonkusale, S. Cost-Effective Wireless Sensors for Detection of Package Opening and Tampering. *IEEE Access* **2020**, *8*, 117122–117132. [[CrossRef](#)]
22. Asci, C.; Wang, W.; Sonkusale, S. Security Monitoring System Using Magnetically-Activated RFID Tags. In Proceedings of the IEEE Sensors, Rotterdam, The Netherlands, 25–28 October 2020.
23. Jani, J.; Leary, M.; Subic, A.; Gibson, M. A review of shape memory alloy research, applications and opportunities. *Mater. Des.* **2014**, *56*, 1078–1113.
24. Wang, W.; Zeng, W.; Sonkusale, S. Tunable Radio Frequency Antenna Using Material Programming. *ACS Appl. Mater. Interfaces* **2022**, *in press*.
25. Riccio, A.; Napolitano, C.; Sellitto, A.; Acanfora, V.; Zarrelli, M. Development of a Combined Micro-Macro Mechanics Analytical Approach to Design Shape Memory Alloy Spring-Based Actuators and Its Experimental Validation. *Sensors* **2021**, *21*, 5506. [[CrossRef](#)]
26. Riccio, A.; Saputo, S.; Zarrelli, M.; Sellitto, A.; Napolitano, C.; Acanfora, V. Shape Memory Alloy-based actuator: Experimental and modelling. In Proceedings of the 2021 IEEE 8th International Workshop on Metrology for AeroSpace, Naples, Italy, 23–25 June 2021; pp. 665–671.
27. Balanis, C. *Antenna Theory Analysis Furthermore, Design*, 3rd ed.; Wiley: Hoboken, NJ, USA, 2005.
28. Taha, O.M.A.; Bahrom1, M.B.; Taha, O.Y.; Aris, M.S. Experimental study on two way shape memory effect training procedure for nitinol shape memory alloy. *ARPJ. Eng. Appl. Sci.* **2015**, *10*, 7847–7851.